Inorganica Chimica Acta 362 (2009) 2770–2775

Contents lists available at ScienceDirect

Inorganica Chimica Acta

journal homepage: www.elsevier.com/locate/ica

Coordination characteristics of di-*O*-picolyl derivative of 1,1′-methylene-bis(2-naphthol): First crystal structure of a monomeric Cu(II) complex of bis{2-[(pyridin-2-yl)methoxy] naphthalen-1-yl}methane

Garima Singh Baghel, Shaikh M. Mobin, Chebrolu P. Rao *

Bioinorganic Laboratory, Department of Chemistry, Indian Institute of Technology Bombay, Powai, Mumbai 400 076, India

ARTICLE INFO

Article history:
Received 24 July 2008
Received in revised form 10 December 2008
Accepted 16 December 2008
Available online 25 December 2008

Keywords:
Di-derivatives of 1,1′-methylene-bis(2-naphthol)
Bis{2-[(pyridin-2-yl)methoxy] naphthalen-1-yl}methane
Monomeric Cu^{2+} complex
Axially elongated octahedral Cu^{2+} center
Helical structure

ABSTRACT

Monomeric Cu(II) complex of bis{2-[(pyridin-2-yl)methoxy] naphthalen-1-yl}methane (L) having a composition, $\{[Cu(L)(H_2O)(ClO_4)](ClO_4)(CH_3OH)_2\}$ (**1**) has been synthesized and characterized by analytical, spectral and magnetic methods and the structure has been established for the first time based on single crystal XRD. The Cu^{2+} center shows axially elongated octahedron with a bound water and perchlorate moieties, where two of the coordinations were long but within the van der Waals distance. The bound water, perchlorate ions and the methanol of crystallization are primarily responsible for the formation of extended lattice structure resulted from the intra-helical interactions. Complex **1** exhibit catecholase activity as studied using 3,5-di-*tert*-butyl catechol.

1. Introduction

Methylene bridged molecular system, such as, 1,1′-methylene-bis-naphthol (**mbn**) or its derivatives exhibit structures where the pendant arms are oriented in *trans*-like fashion. Such orientation is well suited for forming polymeric structures when complexed with metal ions. However, the experimental observations reveal that when each of the aromatic ring is mono-derivatized, the corresponding derivatives yield monomeric complexes rather than the expected polymeric one [1,2]. On the other hand, when the **mbn** is di-derivatized on each of its aromatic ring, viz., 2,3- and 2′,3′-, like that in the pamoic acid, that possesses additional –COOH groups, the resulting metal ion complexes are no more monomeric but tend to be mainly oligomeric or polymeric in nature [3–6]. The monomeric complexes involving directly the **mbn**-moiety (excluding those of the phosphorous derivatives) are rather sparse and includes W(VI) [1] and Ti(IV) [2]. Therefore, it is of great relevance and importance to the development of the coordination chemistry of such molecular systems, viz., **mbn**-derivatives. In the present communication we demonstrate, for the first time, a Cu(II) complex of di-picolyl derivative of **mbn**, viz., bis{2-[(pyridin-2-yl)-methoxy] naphthalen-1-yl}methane (L, Fig. 1) possessing Cu(II) center with tetragonal elongation having both water and perchlorate species bound in the primary coordination sphere.

2. Experimental

2.1. General

All the solvents were purified and dried before use by standard procedures. FTIR spectra were recorded on an Impact 400 Nicolet machine in KBr matrix. C, H and N analysis were performed on a Carlo Erba 1106 elemental analyzer and that of the copper content was estimated using ICP-AES. The ^1H and ^{13}C NMR spectra were recorded on a Varian 400S spectrometer in $CDCl_3$ or DMSO-d_6. UV–Vis spectra were obtained on a Shimadzu UV-260 or UV-2101PC spectrophotometer. The fluorescence emission spectra were recorded on a Perkin-Elmer LS 55 spectrofluorimeter. Magnetic susceptibility measurements were performed on a PAR vibrating sample magnetometer. The EPR measurements were made on a Varian model 109C E-line X-band spectrometer fitted with a quartz dewar for measurements at 77 K (liquid nitrogen), where the spectra were calibrated using tetracyanoethylene (tcne). Single crystal X-ray diffraction data were collected on an OXFORD DIFFRACTION XCALIBUR-S CCD system by ω–2θ scan mode and the absorption corrections were applied by using multi-Scan method. The structure was solved by direct methods SHELXS-97 and refined by full-matrix least squares against F^2 using SHELXL-97 software [7].

* Corresponding author. Tel.: +91 22 2576 7162; fax: +91 22 2572 3480.
E-mail addresses: cprao@iitb.ac.in, cprao@chem.iitb.ac.in (C.P. Rao).

0020-1693/$ - see front matter © 2008 Elsevier B.V. All rights reserved.
doi:10.1016/j.ica.2008.12.019

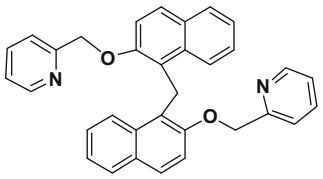

Fig. 1. Schematic representation of the structure of L.

Non-hydrogen atoms were refined with anisotropic thermal parameters. All the hydrogen atoms were geometrically fixed and allowed to refine using a riding model.

2.2. Synthesis and characterization of L

N,*N*-dimethylformamide (160 mL) was taken in a two necked flask fitted with a nitrogen inlet and a reflux condenser. To this **mbn** (4.2 g, 14 mmol); K_2CO_3 (9.66 g, 70 mmol) and 2-picolylchloride hydrochloride (6.9 g, 56 mmol) were added and the reaction mixture was heated at 60–70 °C under nitrogen atmosphere for 12 h. The reaction mixture was then cooled to room temperature, and was poured into water and extracted with $CHCl_3$. The chloroform layer was washed twice with water and dried over anhydrous $NaHSO_4$. The filtrate was evaporated under vacuum (45–50 °C) to dryness and the residue was washed with petroleum ether. Orange solid product (L) formed was crystallized from $CHCl_3/CH_3OH$ to give pale orange crystals. Yield: 5.4 g (80%, based on **mbn**); m.p. 134–137 °C. *Anal.* Calc. for $C_{33}H_{26}O_2N_2$: C, 82.16; H, 5.39; N, 5.81. Found: C, 81.91; H, 5.59; N, 5.59%. ^{1}H NMR ($CDCl_3$, ppm): 8.578 (d, 2H, Py–H); 8.285 (d, 2H, Nap–H); 7.722 (m, 4H, Nap–H); 7.494 (dt, 2H, Py–H); 7.285 (m, 6H, Nap–H); 7.134 (m, 4H, Py–H); 5.265 (s, 4H, Py–CH_2–); 5.148 (s, 2H, Nap–CH_2–Nap). ^{1}H NMR (DMSO-d_6, ppm): 8.590 (d, 2H, Py–H); 8.166 (d, 2H, Nap–H); 7.775 (m, 7H, Nap–H + Py–H); 7.539 and 7.457 (two d, 5H, Py–H + Nap–H); 7.321 (t, 2H, Py–H); 7.237 (m, 5H, Nap–H + Py–H); 5.265 (s, 4H, Py–CH_2–); 5.148 (s, 2H, Nap–CH_2–Nap). ^{13}C NMR ($CDCl_3$, δ ppm): 21.9 (Nap–CH_2–Nap), 71.9 (Py–CH_2–). ESI MS: m/z (%), 483 (100, $(M+1)^+$). Absorption spectral data for L in MeOH in terms of λ_{max}/nm (ε/l mol^{-1} cm^{-1}): 238 (1265), 282 (464), 293 (404), 323 (191), 335 (221).

2.3. Synthesis and characterization of Cu(II) complex, *1*

L (0.48 g, 1.0 mmol) was taken in 25 mL of chloroform to which a methanolic solution of $Cu(ClO_4)_2 \cdot 6H_2O$ (0.365 g, 1.0 mmol, 25 mL) was added (*Caution: Since the perchlorate salts are potentially explosive, these should be used in small portions with great care!*) The reaction mixture was allowed to stir for 3–4 h during which the color of the solution changed from yellow to brown. The filtered solution was kept in the refrigerator wherein nice crystalline compound was separated out within about 3 days and the crystals were found to be suitable for X-ray diffraction. Yield: 0.160 g (26%); m.p. 178–180 °C. *Anal. Calc.* for $C_{35}H_{36}Cl_2CuN_2O_{13}$: C, 50.82; H, 4.39; N, 3.39; Cu, 7.68. Found: C, 50.14; H, 4.68; N, 3.89; Cu, 7.58%. Selected IR bands (KBr, cm^{-1}): 3457(s), 1614(s), 1510(s), 1107(s). Absorption data in MeOH in terms of λ_{max}/nm (ε/l mol^{-1} cm^{-1}): 241 (19190), 261 (18187), 283 (13813), 322 (5048), 335 (5145), 462 (213), 487 (177), 732 (50).

When similar synthetic reactions were carried out using copper nitrate, copper chloride and copper acetate, it is only the ligand that crystallized from the reaction mixtures and not the complex. Experiments carried out under varying ratios of ligand to the metal ion still resulted in 1:1 complex. Further, the synthesis carried out using methanol–acetonitrile and methanol–dichloromethane yielded only the crystals of the ligand and not the complex.

2.4. Experimental details for kinetic measurements

The kinetics of the oxidation of 3,5-di-*tert*-butylcatechol (3,5-dtbc) were determined by the method of initial rates. For this purpose 150 μL of 0.80×10^{-3} M (Effective concentration = 40 μM)solutions of **1** in methanol was treated with 150 μL of 80×10^{-3}, 64×10^{-3}, 48×10^{-3}, 32×10^{-3}, 16×10^{-3} M of 3,5-dtbc solutions in methanol i.e. the complex to substrate ratios was 1:100, 1:80, 1:60, 1:40, 1:20, respectively. The growing band at 395–400 nm of the product 3,5-di-*tert*-butylquinone (3,5-dtbq) has been monitored by UV–Vis spectroscopy. The average initial rates over five independent measurements were determined by linear regression from the slope of the concentration versus time plots. Kinetic parameters were determined from the double reciprocal Lineweaver–Burk plot.

3. Results and discussion

The ligand, bis{2-[(pyridin-2-yl)methoxy] naphthalen-1-yl} methane (L) and its Cu(II) complex, **1**, have been synthesized and characterized as given in Section 2. Complexation of L with Cu^{2+} has also been studied by varying the anion of the copper(II) salt, the ligand to metal ratio and the solvent system, as given in Section 2. The chloride, nitrate and acetate salts of Cu(II) did not yield the complex. However, varying ratios of the ligand to copper perchlorate resulted only in the 1:1 complex. Syntheses carried out in methanol-acetonitrile and methanol-dichloromethane yielded no complex.

3.1. Characterization of *1*

The absorption spectrum of the complex **1** shows characteristic differences from that of L (Fig. 2a) by exhibiting ligand to metal charge transfer as well as d → d transition bands in case of **1** as can be noted from the data given in Section 2. While L shows good fluorescence at around 356 nm upon exciting the sample at 280 nm, the complex **1** exhibit very low intensity owing to the binding of paramagnetic Cu(II) to L as can be seen from Fig. 2b.

Comparison of the ^{1}H NMR spectrum of L with that of **1** clearly indicate the formation of the complex as it reflects in the line broadening of the latter (Fig. 3a) owing to the paramagnetic nature of Cu^{2+}. The aromatic including the pyridyl peaks observed in 7.2–8.6 ppm in case of L were broadened as well as up-field shifted to 7.0–8.2 ppm in **1**. The line broadening were mainly seen with the protons of the pyridyl moiety as well as the methylene group of the arm indicating that the binding of Cu^{2+} is through pyridyl nitrogen and the ether oxygen. The X-band EPR spectrum (Fig. 3b) of **1** in frozen acetonitrile displayed axial distortion of the N_2O_4 coordination sphere with four line spectrum ($g_{||} = 2.29$; $g_{\perp} = 2.08$) exhibiting hyperfine splitting constant of $A_{||} = 143$ G. The crystal structure of **1** reported in this paper indeed confirms the coordination features.

The cyclic voltammogram of **1** exhibit a well defined redox wave for Cu^{II}/Cu^{I} with ΔE_p of 98 mV and a current ratio of 0.84 (Fig. 4a). Since the ΔE_p and the current ratio found in case of the ferrocene–ferrocenium couple were 97 mV and 0.78, respectively, under similar experimental conditions, the redox wave exhibited by **1** can be considered reversible.

3.2. Magnetic studies

Complex **1** exhibited a room temperature magnetic moment of 1.78 BM. However, upon decreasing the T of the sample there is no considerable change observed in χ from RT till about 100 K. However, when the temperature was brought down to 25 K, there is a

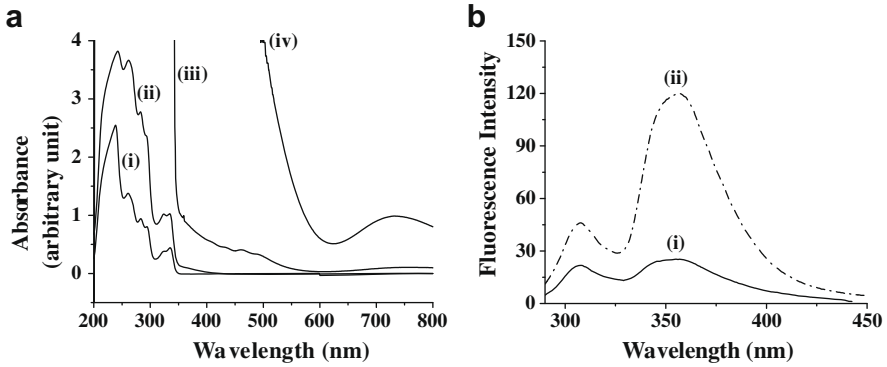

Fig. 2. (a) Absorption spectra measured in methanol: (i) L, 2 mM; (ii) **1**, 0.2 mM, (iii) **1**, 2 mM and (iv) **1**, 20 mM. (b) Fluorescence spectra measured in methanol at 2 μM concentration: (i) **1** and (ii) L.

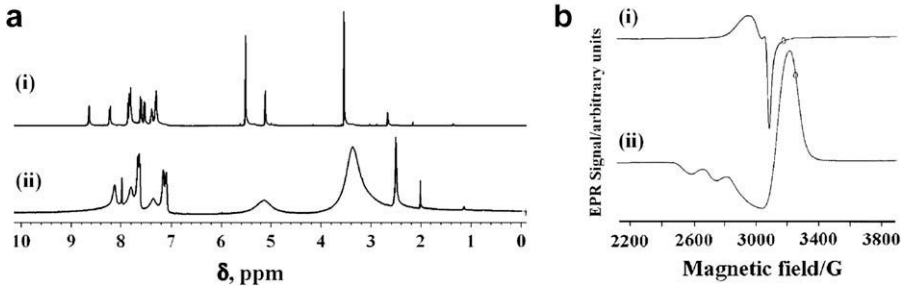

Fig. 3. (a) ^{1}H NMR spectra measured in DMSO-d_6 at 400 MHz: (i) L and (ii) **1**. (b) EPR spectra of **1**: (i) in powder at RT and (ii) in acetonitrile solution frozen at 77 K.

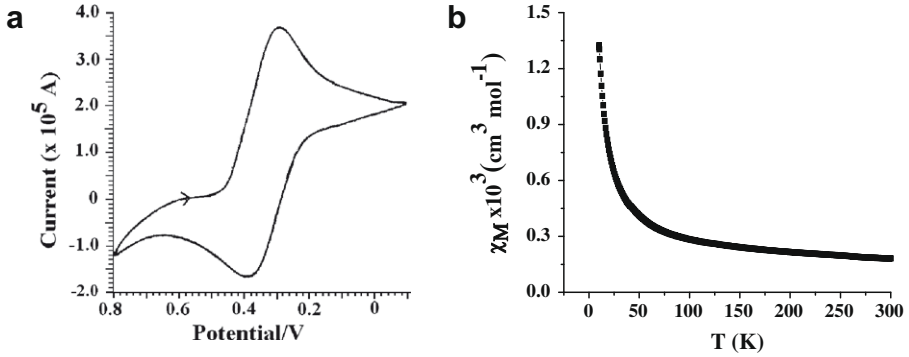

Fig. 4. (a) Cyclic voltammogram of **1** in acetonitrile. (b) Variable temperature magnetic susceptibility data for **1**.

considerable change in the χ value and a very sharp increase was observed below 30 K down to 4 K (Fig. 4b). Thus while **1** is primarily paramagnetic in nature, at temperatures below 25 K it exhibits weak ferromagnetic character. This may be attributed to the helical structure observed for **1** that extends through out the lattice, as discussed later in this paper.

3.3. Crystal structure

Compound **1** crystallizes in monoclinic with space group $P2_1/c$ with a composition of $\{[CuL(H_2O)(ClO_4)](ClO_4)(CH_3OH)_2\}$ as established from single crystal XRD. Preliminary crystallographic data has been summarized in Table 1. The molecular structure of **1** (Fig. 5a) exhibited a six coordinated N_2O_4 binding core where L acts as a tetra-dentate ligand using its two pyridyl nitrogens and two ether 'O', and a water molecule and a perchlorate oxygen. Both the pendant arms are involved in binding to the same Cu(II) center resulting in a mononuclear complex that has no precedence in the literature. Thus the complex unit in **1** is mono-cation and the charge is compensated by the presence of additional perchlorate moiety present in the lattice. Metric data corresponding to this structure has been given in Tables 2 and 3. Though the observed bond lengths and bond angles are normal with the organic moiety, the coordination sphere exhibited distorted octahedral geometry. Distortion from octahedra results from the weak binding of one of the ether oxygens (O2) and one of the perchlorate oxygens (O7) by exhibiting distances of 2.526(2) and 2.559(3) Å respectively for $Cu^{2+}\cdots O2$ and $Cu^{2+}\cdots O7$, and $O2\cdots Cu^{2+}\cdots O7$ angle of 156.1(1)°. These distances are certainly higher than that for a covalent bond, but are much below the sum of the van der Waals radii (2.78 Å). The other two trans angles, viz., 152.9(1)° and 167.1(1)° are also indicative of the distortion in the Cu(II) geometry. Thus in **1**, the Cu(II) center effectively exhibits a pseudo six-coordination geometry leading to a highly distorted octahedral one with elongated axial bonds as expected for a d^9 system and this is being supported by the absorption and EPR data. The coordination sphere

Table 1
Crystal data and structure determination parameters for **1**.

Formula	$[Cu(L)(H_2O)(ClO_4)](ClO_4)(CH_3OH)_2$
Composition	$C_{35}H_{36}Cl_2CuN_2O_{13}$
Formula weight	827.10
T (K)	120(2)
Wavelength (Å)	0.71073
Crystal system, space group	monoclinic, $P21/c$
Crystal size (mm^3)	$0.36 \times 0.33 \times 0.21$
a, (Å)	13.160(1)
b (Å)	12.790(3)
c(Å)	22.138(3)
β (°) ,	105.3(1)
Volume ($Å^3$)	3593.9(10)
Z	4
ρ_{calc} ($g\ cm^{-3}$)	1.529
μ (mm^{-1})	0.826
$F(000)$	1708
θ Range (°)	3.19–25.00
Reflections collected	28 863
Unique reflections	6315
R_{int}	0.0344
Absorption correction	semi-empirical
Maximum and minimum transmission	0.8456 and 0.7552
Data/restraints/parameters	6315/0/496
Goodness-of-fit (GOF) on F^2	1.028
Final R indices [$I > 2\sigma(I)$]	$R_1 = 0.0411$, $wR_2 = 0.1089$
R indices (all data)	$R_1 = 0.0604$, $wR_2 = 0.1180$
Max. & min. $\Delta\rho$ ($e\ Å^{-3}$)	0.642, −0.652

Weight factor, $w = 1/[\sigma(F_o^2) + (0.1403P)^2]$ where $P = (F_o^2 + 2F_c^2)/3$.

and the conformation of L present in the complex **1** can be clearly seen from the stereoview given in Fig. 5b.

3.4. Lattice structure

The presence of several units, such as, bound water, bound and unbound perchlorates, two methanols, are responsible for the inter connectivity of the complex units to result in a complicated three-dimensional lattice structure. The data for the hydrogen bonds present in the lattice has been given in Table 4. The formation of such lattice structure can be visualized as follows: (i) Hydrogen bonded net work formed between the unbound perchlorate of one of the units with the bound water of one of the neighbour units via its methanol molecules results in a dimer wherein the net work has a 10-membered cycle with four-H-bonds present in it (Fig. 6a). (ii) Each unit of such dimer further interacts with appropriate neighbour dimer units via mutually formed two –C–H···O hydrogen bonds, wherein the –C–H is drawn from the pyridyl moiety and the O is drawn from the bound perchlorate (Fig. 6b). (iii) Each of the two oxygens of the free perchlorate unit mentioned under (i) further interacts (Fig. 6c) through two different dimers via O···H–C interactions while in one case the C–H is drawn from the pyridyl, in the other it is drawn from the picolyl $–CH_2$. While the combination of (i) and (ii) results in the formation of a helical chain (Fig. 7), this extends further to result in a three-dimensional connectivity in the lattice when one considers the interactions mentioned under (iii). Thus the complex units are extensively inter-connected to form a three-dimensional net work as a result of the presence of perchlorate units. Such inter-connectivity among the complex units seems to be responsible for the sudden increase in the magnetic susceptibility observed at temperatures below 25 K.

3.5. Catecholase activity

Catalytic oxidation of **1** on the commonly used model substrate, 3,5-di-*tert*-butylcatechol (3,5-dtbc) at room temperature in methanolic solution was monitored by means of UV–Vis spectroscopy by following the changes observed in the absorbance of 395–400 nm band arising from the resulting quinone product, wherein it shows a saturation kinetics (Fig. 8a and b). The catalyst **1** used was 40 μM. Control studies were carried out with simple 3,5-dtbc, {3,5-dtbc + L} and $Cu(ClO_4)_2 \cdot 6H_2O$ under similar experimental

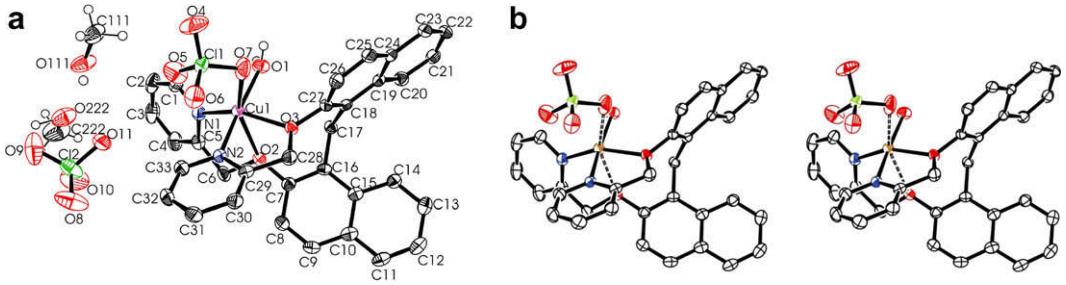

Fig. 5. (a) Single crystal XRD structure of **1** showing both the cationic and anionic portions as ORTEP. Hydrogens are not shown for clarity except for methanol and water. (b) Stereoview of the cationic complex species in **1**.

Table 2
Bond distances (Å) observed based on X-ray structure of **1**.

Cu(1)–O(1)	1.911(2)	C(2)–C(3)	1.383(5)	C(22)–C(23)	1.364(4)	C(20)–C(21)	1.367(4)
Cu(1)–N(2)	1.963(2)	C(3)–C(4)	1.383(5)	C(23)–C(24)	1.416(4)	C(18)–C(19)	1.416(4)
Cu(1)–N(1)	2.002(2)	C(4)–C(5)	1.391(4)	C(24)–C(25)	1.409(4)	9(4)C(21)	1.408(4)
Cu(1)–O(3)	2.063(2)	C(5)–C(6)	1.490(4)	C(25)–C(26)	1.490(4)	N(2)–C(33)	1.348(4)
Cu(1)–O(2)	2.526(2)	C(7)–C(16)	1.380(4)	C(26)–C(27)	1.411(4)	C(19)–C(24)	1.436(4)
Cu(1)–O(7)	2.559(4)	C(7)–C(8)	1.414(4)	C(28)–C(29)	1.504(4)	C(18)–C(27)	1.372(4)
Cl(1)–O(4)	1.407(3)	C(8)–C(9)	1.361(4)	C(29)–C(30)	1.380(4)	N(2)–C(29)	1.350(4)
Cl(1)–O(5)	1.433(2)	C(9)–C(10)	1.412(4)	C(30)–C(31)	1.389(4)	C(19)–C(20)	1.425(4)
Cl(1)–O(6)	1.433(2)	C(10)–C(11)	1.421(4)	C(31)–C(32)	1.384(5)	N(1)–C(5)	1.364(4)
Cl(1)–O(7)	1.440(2)	C(10)–C(15)	1.422(4)	C(32)–C(33)	1.377(4)	C(17)–C(18)	1.530(4)
Cl(2)–O(8)	1.411(3)	C(11)–C(12)	1.363(5)	C(1)–C(2)	1.391(3)	C(11)–C(12)	1.382(4)
Cl(2)–O(10)	1.431(3)	C(13)–C(14)	1.369(4)	O(2)–C(6)	1.435(3)	C(16)–C(17)	1.521(4
Cl(2)–O(11)	1.437(2)	C(14)–C(15)	1.430(4)	O(3)–C(27)	1.412(3)	N(1)–C(1)	1.412(3)
Cl(2)–O(9)	1.460(3)	C(15)–C(16)	1.425(4)	O(3)–C(28)	1.440(3)		

Table 3
Bond angles (°) observed based on the X-ray structure of **1**.

N(1)–Cu(1)–N(2)	99.1(1)	O(2)–C(7)–C(8)	21.3(3)	N(2)–C(33)–C(32)	122.4(3)
N(1)–Cu(1)–O(1)	92.9(1)	C(9)–C(8)–C(7)	119.8(3)	C(33)–C(32)–C(31)	119.0(3)
N(1)–Cu(1)–O(2)	72.8(1)	C(8)–C(9)–C(10)	121.1(3)	C(4)–C(5)–C(6)	121.0(3)
N(1)–Cu(1)–O(3)	152.9(1)	C(16)–C(7)–O(2)	116.9(2)	C(32)–C(31)–C(30)	118.8(3)
N(1)–Cu(1)–O(7)	131.1(1)	C(9)–C(10)–C(11)	121.7(3)	N(1)–C(5)–C(4)	120.9(3)
N(2)–Cu(1)–O(1)	167.1(1)	O(2)–C(6)–C(5)	107.4(2)	C(29)–C(30)–C(31)	119.4(3)
N(2)–Cu(1)–O(2)	87.7(1)	C(9)–C(10)–C(15)	118.8(3)	C(30)–C(29)–C(28)	120.3(3)
N(2)–Cu(1)–O(3)	80.7(1)	C(11)–C(10)–C(15)	119.5(3)	C(3)–C(4)–C(5)	119.6(3)
N(2)–Cu(1)–O(7)	87.9(1)	C(12)–C(11)–C(10)	121.4(3)	N(2)–C(29)–C(28)	118.0(2)
O(1)–Cu(1)–O(2)	100.6(1)	C(11)–C(12)–C(13)	119.7(3)	C(4)–C(3)–C(2)	119.2(3)
O(1)–Cu(1)–O(3)	90.8(1)	C(13)–C(14)–C(15)	121.6(3)	C(1)–C(2)–C(3)	121.7(3)
O(2)–Cu(1)–O(3)	80.2(1)	C(10)–C(15)–C(16)	120.1(3)	O(3)–C(28)–C(29)	108.8(2)
O(2)–Cu(1)–O(7)	156.1(1)	C(10)–C(15)–C(14)	117.5(3)	N(1)–C(1)–C(2)	122.6(3)
O(3)–Cu(1)–O(7)	75.9(1)	C(16)–C(15)–C(14)	122.3(3)	C(27)–O(3)–C(28)	115.5(2)
C(1)–N(1)–Cu(1)	120.3(2)	C(7)–C(16)–C(15)	118.4(3)	O(3)–C(27)–C(26)	117.7(2)
C(5)–N(1)–Cu(1)	120.6(2)	C(7)–C(16)–C(17)	121.2(3)	C(7)–O(2)–C(6)	118.0(2)
C(27)–O(3)–Cu(1)	125.5(2)	C(15)–C(16)–C(17)	120.5(2)	C(18)–C(27)–C(2)	123.9(3)
C(28)–O(3)–Cu(1)	114.8(2)	C(16)–C(17)–C(18)	115.9(2)	C(18)–C(27)–O(3)	118.2(2)
C(29)–N(2)–Cu(1)	116.4(2)	C(27)–C(18)–C(19)	117.2(2)	C(29)–N(2)–C(33)	118.6(2)
C(33)–N(2)–Cu(1)	124.3(2)	C(27)–C(18)–C(17)	120.7(2)	C(25)–C(26)–C(27)	119.0(3)
O(4)–Cl(1)–O(5)	109.8(2)	C(19)–C(18)–C(17)	121.9(2)	C(1)–N(1)–C(5)	118.8(3)
O(4)–Cl(1)–O(6)	110.8(2)	C(20)–C(19)–C(24)	116.8(3)	C(26)–C(25)–C(24)	120.9(3)
O(5)–Cl(1)–O(6)	109.0(2)	C(20)–C(19)–C(18)	123.6(3)	O(11)–Cl(2)–O(9)	108.2(2)
O(4)–Cl(1)–O(7)	111.4(2)	C(24)–C(19)–C(18)	119.6(3)	C(23)–C(24)–C(19)	120.0(3)
O(5)–Cl(1)–O(7)	107.0(2)	C(21)–C(20)–C(19)	121.3(3)	O(10)–Cl(2)–O(9)	108.1(2)
O(6)–Cl(1)–O(7)	108.7(2)	C(20)–C(21)–C(22)	121.3(3)	C(25)–C(24)–C(19)	119.5(3)
O(8)–Cl(2)–O(10)	112.4(2)	C(23)–C(22)–C(21)	119.4(3)	O(8)–Cl(2)–O(9)	107.7(2)
O(8)–C1(2)–O(11)	09.9(2)	C(22)–C(23)–C(24)	121.2(3)	O(10)–Cl(2)–O(11)	110.5(2)
C(25)–C(24)–C(23)	120.6(3)				

Table 4
Hydrogen bond data in case of **1**.

D–H···A	*d*(D–H) (Å)	*d*(A···H) (Å)	*d*(D···A) (Å)	*d*(D···A) (Å)
O111–H102···O11	0.62	2.239	2.811	155.7
O1–H101···O111	0.70	1.870	2.569	174.1
O1–H102···O222	0.83	1.839	2.637	161.9
C111–H11···O5	0.96	2.460	3.282	143.5
C31–H31···O6	0.93	2.487	3.411	172.2
C33–H33···O11	0.93	2.433	3.303	155.7

conditions. Comparison of the observed data with that of these controls clearly indicate the positive role played by **1** in the oxidation of 3,5-dtbc.

In the first 100 min, the percent of substrate reacted has been estimated to be 57%, 32%, 24%, 17% and 14%, respectively, at the concentrations of the substrate used, viz., 1:20, 1:40, 1:60, 1:80 and 1:100, while the concentration of **1** has been maintained same in all the cases. The initial rates obtained based on logarithmic plots for all the five different 3,5-dtbc mole ratios were fitted to

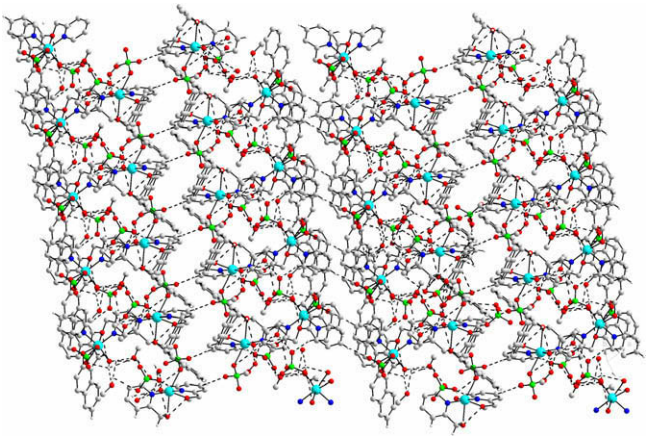

Fig. 7. Lattice structure of **1** indicating helical arrangement of Cu(II) centers present in the column and the inter-column interactions.

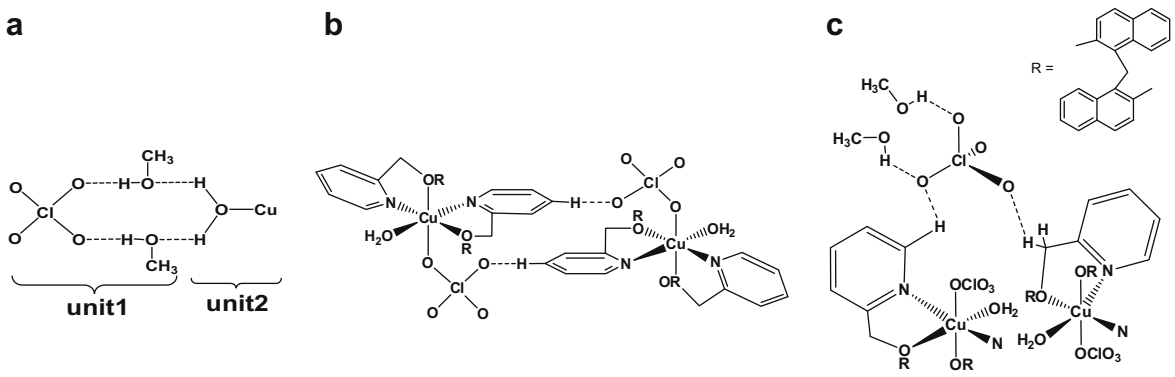

Fig. 6. (a) Formation of dimeric unit; (b) interaction between the two dimers; and (c) interactions formed through free perchlorate moiety in the lattice.

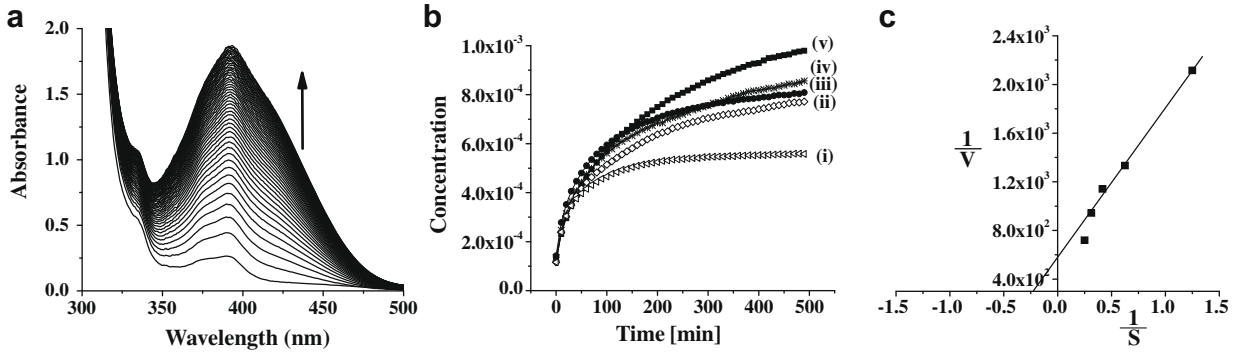

Fig. 8. Oxidation of 3,5-dtbc by **1** in methanol: (a) Absorption spectral traces of 4 mM of 3,5-dtbc in the presence of 40 μM of **1**. (b) Plot of absorbance at 395–400 nm vs. time at five different ratios of 1 to 3,5-dtbc: (i) 1:20; (ii) 1:40; (iii) 1:60;: (iv) 1:80; (iii) 1:100. (c) Lineweaver–Burk plot for the studies reported in (b). Units for 1/V are (mol^{-1} L min). The *x*-axis is 1/S ($x10^3$ mol L^{-1}).

Lineweaver–Burk plots (Fig. 8c) to give the kinetic parameters. This was found to have a turn over number (TON) of 16 ± 1 for a reaction period of 100 min, with K_m and K_{cat} being 2.17×10^{-3} M and 2497.5 min^{-1}, respectively. The TON value observed in the present case is well within the range observed by a number of mono- and dinuclear copper complexes reported in the literature [8–19].

4. Conclusions

Di-derivatization of 1,1′-methylene-bis(2-naphthol) using picolyl end groups at the pendant arms resulted in hemi-calix[4] naphthalene derivative L, bis{2-[(pyridin-2-yl)methoxy] naphthalen-1-yl}methane, which yields crystalline product with Cu(II), **1**. This is one among very few crystal structures known of the metal ion the complexes of **mbn** or its derivatives and certainly the first one on the copper. The Cu(II) exhibits an axially elongated and highly distorted octahedral geometry where the ligand acts as a neutral, tetradentate one wherein the coordination sphere possesses water and perchlorate moieties. The helical network of the complex units formed in the lattice, using perchlorate, methanol and water moieties as linkers, is responsible for the sudden increase in the observed magnetic susceptibility below 25 K. Complex, **1** also exhibits catecholase activity as studied using 3,5-dtbc.

Acknowledgments

C.P.R. acknowledges the financial support from DST and CSIR, New Delhi and DAE, Mumbai for financial support. G.S.B. acknowledges the senior research fellowship from CSIR, New Delhi. We thank the DST's National Single Crystal X-ray Diffraction Facility, IIT Bombay for providing the data.

Appendix A. Supplementary material

CCDC 711525 contains the supplementary crystallographic data for this paper. These data can be obtained free of charge from The Cambridge Crystallographic Data Centre via www.ccdc.cam.ac.uk/data_request/cif. Supplementary data associated with this article can be found, in the online version, at doi:10.1016/j.ica.2008.12.019.

References

[1] A. Lehtonen, R. Sillanpa, Polyhedron 2 (2002) 1017.
[2] P.V. Rao, C.P. Rao, E.K. Wegelius, E. Kolehmainen, K. Rissanen, J. Chem. Soc., Dalton Trans. (1999) 4469.
[3] D.A. Haynes, J. Van de Streek, J.C. Burley, W. Jonesa, W.D. Sam Motherwell, Acta Crystallogr. Sect. E62 (2006) 1170.
[4] D.A. Haynes, W. Jones, W.D. Samuel Motherwell, Cryst. Eng. Commun. 7 (2005) 538.
[5] J.-J. Wang, M.-L. Yang, H.-M. Hu, G.-L. Xue, D.-S. Li, Q.-Z. Shi, Inorg. Chem. Commun. 10 (2007) 269.
[6] M. Du, C.-P. Li, X.-J. Zhao, Q. Yu, Cryst. Eng. Commun. 9 (2007) 1011.
[7] G.M. Sheldrick, SHELX-97 – A Program for Crystal Structure Solution and Refinement, University of Goettingen, Germany, 1997, Release 97-2.
[8] C. Belle, C. Beguin, I. Gautier-Luneau, S. Hamman, C. Philouze, J.L. Pierre, F. Thomas, S. Torelli, Inorg. Chem. 41 (2002) 479.
[9] S.C. Cheng, H.H. Wei, Inorg. Chim. Acta 340 (2002) 105.
[10] J. Mukherjee, R. Mukherjee, Inorg. Chim. Acta 337 (2002) 429.
[11] S. Mukherjee, T. Weyhermuller, E. Bothe, K. Wieghardt, P. Chaudhuri, Dalton Trans. (2004) 3842.
[12] C. Yang, M. Vetrichelvan, X. Yang, B. Moubaraki, S.K. Murray, J.J. Vittal, Dalton Trans. (2004) 113.
[13] R.A. Peralta, A. Neves, A.J. Bortoluzzi, A.A. Dos, F.R. Xavier, B. Szpoganicz, H. Terenzi, M.C.B. Oliveira, E. Castellano, G.R. Friedermann, A.S. Mangrich, M.A. Novak, J. Inorg. Biochem. 100 (2006) 992.
[14] N.A. Rey, A. Neves, A.J. Bortoluzzi, C.T. Pich, H. Terenzi, Inorg. Chem. 46 (2007) 348.
[15] M.U. Triller, D. Pursche, W-Y Hsieh, V.L. Pecoraro, A. Rompel, B. Krebs, Inorg. Chem. 42 (2003) 6274.
[16] Y. Gultneh, A. Farooq, K.D. Karlin, S. Liu, J. Zubieta, Inorg. Chim. Acta 211 (1993) 171.
[17] D. Kovala-Demertzi, S.K. Hadjikakou, M.A. Demertzis, Y. Deligiannakis, Inorg. Biochem. 69 (1998) 223.
[18] A. Jancso, Z. Paksi, N. Jakab, B. Gyurcsik, A. Rockenbauerd, T. Gajda, Dalton Trans. (2005) 3187.
[19] M.R. Malachowski, M.G. Davidson, Inorg. Chim. Acta 162 (1989) 199.